Effect of Cobratoxin Binding on the Normal Mode Vibration within Acetylcholine Binding Protein

Edward J. Bertaccini,*[,†,‡] Erik Lindahl,[§] Titia Sixma,[||] and James R. Trudell[†]

Department of Anesthesia, Stanford University School of Medicine and Beckman Center for Molecular and Genetic Medicine, Stanford, California 94305-5117, Department of Veterans Affairs, Palo Alto VA Health Care System, Palo Alto, California 94304, Stockholm Bioinformatics Center and Center for Biomembrane Research, Stockholm University, Stockholm, Sweden, and Division of Molecular Carcinogenesis, Netherlands Cancer Institute, Amsterdam, The Netherlands

Received December 07, 2007

Recent crystal structures of the acetylcholine binding protein (AChBP) have revealed surprisingly small structural alterations upon ligand binding. Here we investigate the extent to which ligand binding may affect receptor dynamics. AChBP is a homologue of the extracellular component of ligand-gated ion channels (LGICs). We have previously used an elastic network normal-mode analysis to propose a gating mechanism for the LGICs and to suggest the effects of various ligands on such motions. However, the difficulties with elastic network methods lie in their inability to account for the modest effects of a small ligand or mutation on ion channel motion. Here, we report the successful application of an elastic network normal mode technique to measure the effects of *large* ligand binding on receptor dynamics. The present calculations demonstrate a clear alteration in the native symmetric motions of a protein due to the presence of large protein cobratoxin ligands. In particular, normal-mode analysis revealed that cobratoxin binding to this protein significantly dampened the axially symmetric motion of the AChBP that may be associated with channel gating in the full nAChR. The results suggest that alterations in receptor dynamics could be a general feature of ligand binding.

INTRODUCTION

The nicotinic acetylcholine receptor (nAChR) plays a significant role throughout the human body, regulating a variety of vital functions within both the peripheral and central nervous systems. A much greater understanding of its overall structure has been derived from the cryoelectron microscopy work of Unwin and co-workers on the nAChR from the torpedofish (*Torpedo marmorata*).[1,2] Just as with many other protein receptors and channels, ligand binding to the nAChR significantly alters its function, almost certainly its structure, and quite possibly its dynamics.[3] However, the atomic details of these effects remain an open question since it has not yet been possible to obtain a single high resolution structure of a complete nAChR from X-ray crystallography, not to mention multiple structures of alternative bound states. The first high resolution crystal structure of a protein with significant structural and sequence homology to the extracellular ligand binding domain (LBD) of the nAChR is that of the acetylcholine binding protein (AChBP) from the snail *Lymnaea stagnalis*.[4,5] This protein has lent itself to higher resolution analyses of the atomic interactions responsible for ligand binding as well as the physiologically relevant, large-scale protein motions associated with such binding. Additionally, several crystal structures of AChBP have now been obtained with a variety of bound ligands present. These ligand-bound structures could help us understand the corresponding ligand binding and functional influence within the nAChR. They include carbamoylcholine and nicotine,[6] conotoxin,[7,8] and cobratoxin.[9] In the context of AChBP, ligands such as nicotine are small and nonpeptide in nature, but cobratoxin is a relatively large peptide ligand with predictably significant effects on the AChBP.

Molecular simulation would seem an obvious way to assess the effect of bound ligand on protein dynamics, but since it is not yet possible to simulate molecules that are the size of ion channels and membrane receptors on microsecond timescales, several approximate methods have been developed. One of the first and still most popular approaches is normal-mode analysis, which introduces a harmonic approximation of the energy landscape around a local minimum and breaks down the motion into harmonic eigenmode components by diagonalizing the Hessian matrix.[10–12] This works well for small molecules, but the initial minimization required can lead to structural distortion, and the computational complexity increases rapidly as $O(N^3)$, where N is the number of atoms. Consequently, simplified "elastic network" normal-mode analyses based only on the Cα coordinates have become quite popular and shown to at least qualitatively reproduce important dynamics.[13–17] We have recently developed an all-atom extension to the elastic network algorithms, as described in the Methods section,[18] in order to

* Corresponding author phone: (650)493-5000 ext. 65180; fax: (650)852-3423; e-mail: edwardb@stanford.edu. Corresponding author address: Department of Anesthesia, 112A Palo Alto VA Health Care System, 3801 Miranda Ave., Palo Alto, CA 94304.

† Stanford University School of Medicine and Beckman Center for Molecular and Genetic Medicine.

‡ Palo Alto VA Health Care System.

§ Stockholm University.

|| Netherlands Cancer Institute.

10.1021/ci700456s CCC: $40.75
Published on Web 03/19/2008

better model the atomic detail of the interactions between ligand and receptor where the ligand is *not* protein in nature.

This paper presents the results of all-atom elastic network normal-mode analyses of the large-scale motion of the AChBP, both in the presence and absence of cobratoxin as well as nicotine. As such analyses clearly demonstrate, cobratoxin binding markedly alters the motions of AChBP, an effect that may be relevant to ion channel gating in the full nAChR. A similar elastic network calculation demonstrates, by contrast, that the small *nonprotein* nicotine ligand does not significantly alter large-scale motions described by the elastic network methods. The latter is a result more likely due to the limitations of the technique than to the actual effect of nicotine on ion channels. Alternatively, the lack of nicotine effect here possibly suggests that an agonist does not change the overall nature of the motion itself but that agonist binding simply stabilizes one protein state over another through differential binding affinity, something not demonstrable in a normal-mode analysis.

METHODS

The coordinate files of AChBP without ligand or HEPES buffer molecules (1I9B.pdb and referred to as AChBP), AChBP with 5 bound nicotine molecules (1UW6.pdb and referred to as AChBP+5nic) and of AChBP with 5 bound cobratoxin peptides (1YI5.pdb and referred to as AChBP+5cobra) were obtained from the Research Collaboratory for Structural Biology Protein Data Bank (RCSB PDB).[19] Each file was imported into DS Viewer 5.0 (Accelrys, San Diego, CA) for the appropriate addition of hydrogens as necessary. Versions of each of the aforementioned files without hydrogens were also kept and subsequently tested, as noted below for the effect of hydrogen presence.

So as to further test for the specificity of effect of cobratoxin on AChBP, DS Viewer was used to remove the cobratoxins from 1YI5.pdb (AChBP+5cobra), to create an additional file with no cobratoxins called AChBP+0cobra. Note that AChBP from 1I9B is extremely similar, as noted below, but distinctly different from the AChBP+0cobra derived from 1YI5.pdb.

All of these files were then separately used as input for the Lindahl All-Atom Based Elastic Network (LAABEN) Normal Mode Analysis program, as described in our previous work.[18,20] This algorithm is derived from the purely residue-geometry-based elastic network models[13,14,21] which use simple spring potentials, rather than assigning force-field based interactions to atoms. In principle this is a less detailed model, but it has major advantages in not being sensitive to parametrization details since it only uses the geometry between each atom. Also, by defining the initial configuration as the reference state it avoids any initial energy minimizations that might distort the structure. A slight drawback is that it is not possible to determine absolute frequencies of elastic network modes, but since even frequencies of force-field based modes do not take water damping into account,[13] this is less of an issue. Compared to classical elastic network models that use rigid-body approximation for residues, our use of sparse matrix diagonalization techniques makes it possible to retain *full Cartesian degrees of freedom* for all atoms and obtain accuracy much closer to that of force field based normal-mode analysis[10–12] with a tremendous decrease in resource utilization, as previously reported.[22] In particular, previous work in our laboratory has demonstrated that C-alpha atom based techniques, all-atom based techniques with hydrogens, and all-atom based techniques without hydrogens tend to show very little difference in large scale collective motions of a full scale model of an LGIC.[22] However, we specifically chose to use all-atom normal-mode analysis including hydrogens for the AChBP, AChBP+5cobra, and the AChBP+0cobra to see if there was any effect on normal modes due to the explicit presence of a nonprotein–ligand, namely nicotine, since it has no C-alpha atom construct. Input parameters included the number of normal modes desired for a particular run, an exponential short interaction weight parameter of 2, an interaction cutoff default of 10 Å, and the implementation of a sparse matrix algorithm for matrix diagonalization and storage.

Each of the aforementioned normal-mode calculations produced coordinate trajectory files for analysis. Root-mean-square deviations of each residue were produced from the application of the g_rms analysis utility within the GROMACS software suite[23] to the coordinate trajectory files output from the normal-mode analyses. The rmsd trajectory data were then imported into Microsoft Excel for further analysis and plotting. Initial rmsd of each AChBP complex was performed with Deepview 3.7sp5.[24]

For the purposes of comparing the relevant normal mode trajectories between complexes, the scalar product S of motion vectors were defined by extracting the normal mode components of N exactly matching atoms into new vectors $\mathbf{a}^i$ and $\mathbf{a}^j$ and calculated as

$$S = \sum_{k=1}^{3N} a_k^i a_k^j,$$

where the vectors **a** have been normalized so that the scalar product of a vector with itself is unity.

RESULTS

The backbone structure of AChBP from all three file sources is remarkably similar though not exactly the same. The overall rmsd of the starting AChBP protein backbone compared to AChBP+5nic is 1.03 Å over 4012 matching backbone atoms. Likewise, the overall rmsd of the starting AChBP protein backbone compared to AChBP+5cobra is 1.19 Å over 3880 matching backbone atoms (Figure 1).

The motion present within AChBP that could contribute to dynamics similar to ion channel opening can be described as a "radial blossoming" motion. This is characterized by the axially symmetric, radial vibration of each of the five subunits about the ion pore that they surround. (Figure 2 A−C). AChBP+0cobra actually demonstrates the irislike twisting motion that has been associated with ion channel opening in normal mode calculations of full LGIC models performed by our laboratory as well as the laboratories of others.

Normal mode vectors of the different bound structures were compared by projecting one vector onto another using scalar products of vectors for all matching atoms (see the Methods section for a definition). Based on this, the normal mode of AChBP can be seen as virtually identical to that of AChBP+5nic: a scalar product of $S = 0.95$ indicates the modes are almost perfectly parallel. However, the motion in this same general direction within AChBP+5cobra is

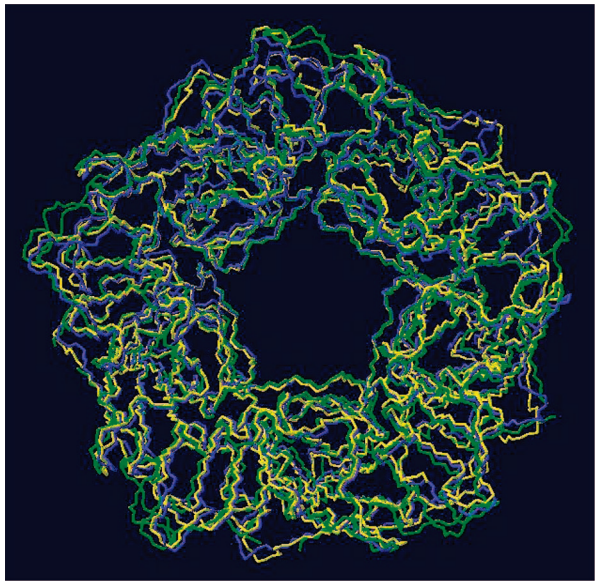

Figure 1. rmsd based alignment of the AChBP backbone from 1I9B (yellow), AChBP+nic from 1UW6 (blue), and AChBP+cobra from 1YI5 (green). Notice the overall excellent alignment of the protein backbone.

dramatically different from that of either of the aforementioned, as demonstrated in a gross dampening of the radial blossoming motion. The vector scalar products of this AChBP+5cobra mode are $S = 0.64$ when compared to the corresponding mode in AChBP and $S = 0.65$ compared to the corresponding AChBP+5nic mode. Figure 3 shows how the per-residue rmsd over the entire vibrational trajectory matches closely between AChBP and AChBP+5nic modes, while AChBP+5cobra deviates significantly.

In fact, in a similar plot that includes the cobratoxin residues, it appears that much of the motion associated with the corresponding normal mode of AChBP+5cobra has been conveyed to a large vibration within each of the five bound cobratoxin molecules instead of the native AChBP itself (Figure 4). Normal mode calculations performed on both the AChBP and AChBP+5cobra but without hydrogens showed nearly identical motions to those calculations performed with hydrogens.

DISCUSSION

For the examination of large-scale protein motions, current computational capabilities allow molecular dynamics simulations only on relatively small proteins. It is not possible to perform large-scale molecular dynamics calculations over the millisecond time scale required for ion channel gating within a 26000 atom ligand gated ion channel (LGIC), even with the most modern of computational hardware. Normal mode analysis breaks down the overall motion within a structure into its individual harmonic components. It is less computationally demanding relative to molecular dynamics and has been shown to produce reasonable approximations of the large amplitude, low frequency motions within proteins.[14,15,25–27] We have recently used normal-mode analysis for the examination of much larger proteins that, relative to the current computational capabilities, were much too big for more detailed methods to handle.[20,22] Concurrent with our work, several other groups have used similar approximate normal mode techniques to calculate the variety of motions present within a large nAChR model,[25,28,29] the potassium channel,[30] and the bacterial mechanosensitive channel.[31] However, none of these protein complexes contain native ligands. Preliminary calculations in our laboratory have shown that merely docking ligands to proteins within putative binding sites does not produce structural changes large enough to alter natural protein motions, as discerned by elastic network based normal mode approximations. It is also questionable whether docking algorithms are accurate enough to bind a ligand in such a way as to reliably produce relevant changes in overall protein structure noticeable by such analyses.

In this paper, we have focused our normal-mode analyses on crystal structures involving AChBP. While this protein is not directly involved in any form of ion conductance, it is homologous to the ligand binding domain of the nAChR that is ubiquitous throughout the nervous system. While the AChBP may offer a wonderful structural template that provides invaluable insight into molecular recognition by nAChRs, some have questioned its validity as a good functional template for ligand-binding dynamics in LGICs.[32,33] Others have found it very useful with regards to making greater inferences about the nAChR itself. Recently, Williamson et al. have used the AChBP as a docking template onto which to model their NMR derived conformation of the acetylcholine ligand itself.[34] However, while coordinates of a nAChR within the torpedofish are available, they are not at the higher resolution present within the AChBP structure, and coordinates of the nAChR with bound ligands are not currently available. In contrast, the AChBP has been crystallized in the presence of a variety of ligands, and high resolution structures have been obtained. Of particular relevance to our studies, superposition of bound and unbound structures clearly demonstrates that ligand binding causes only minimal changes in static tertiary protein structure. This lack of large changes is seen in our rmsd analysis of the AChBP in Figure 1. Therefore, it is possible that the major effect of ligand binding on AChBP is indeed to alter its large-scale dynamics.

Many currently available elastic network models for normal-mode analysis focus solely on peptide backbone structure and are, by definition, unable to account for the presence of nonprotein moieties since they use the C-alpha atoms for their main degrees of freedom. In principle this restriction does not apply to our all-atom based method, but all simplified models are likely to be less sensitive to small ligand perturbations rather than larger peptide effects. Cobratoxin is thus a very interesting example to understand how ligand binding influences large-scale collective dynamics. Additionally, the large size of the cobratoxin ligand was sufficient, even without hydrogens, to clearly demonstrate an effect.

In contrast, it is clear from the calculation on AChBP+5nic, which contains five small bound nicotine molecules, that *even* our all-atom elastic network calculation (LAABEN) cannot demonstrate any significant alterations in normal modes due to the presence of ligand. This problem is most likely due to current shortcomings of the simplified models and does not imply that nicotine binding does not have an effect on protein dynamics. Furthermore, it appears that the addition of hydrogens could not further elicit such an effect from the small nicotine ligands. However, an alternative explanation

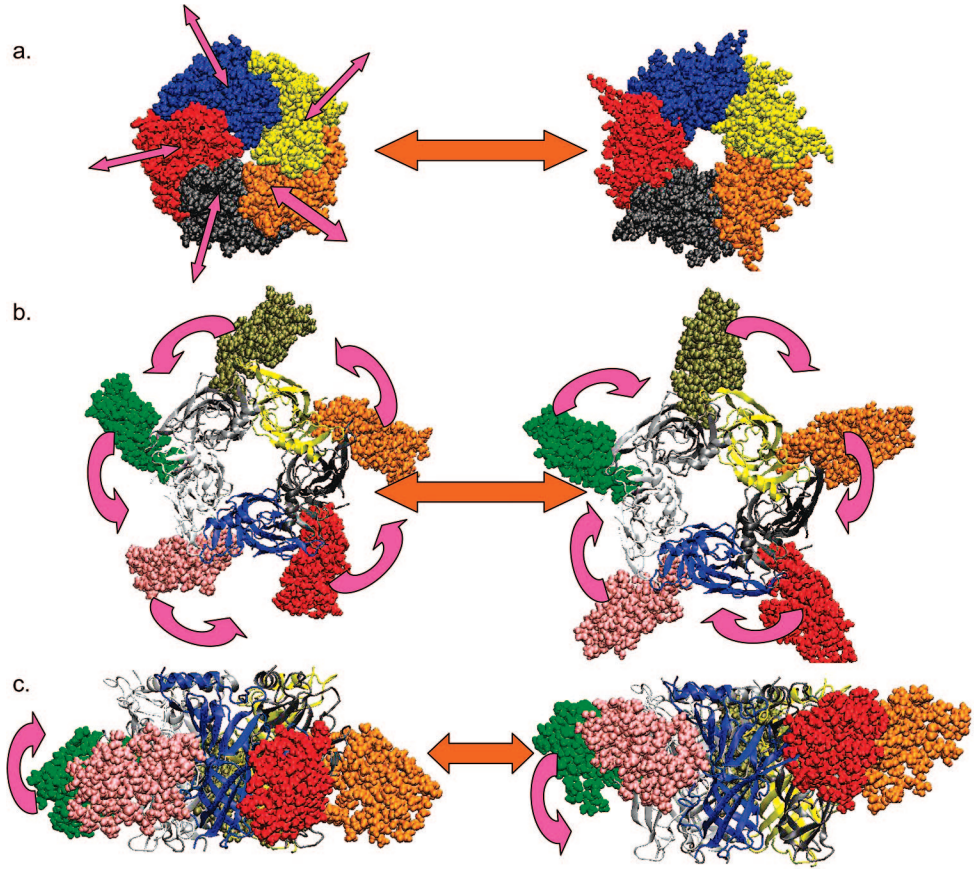

Figure 2. (a) The "radial blossoming motion within native AChBP associated with possible LGIC gating. The top view (b) and side view (c) of the comparable normal mode within 1YI5. Notice the lack of AChBP motion and the much exaggerated "wagging" motion of the bound cobratoxin in the two directions noted.

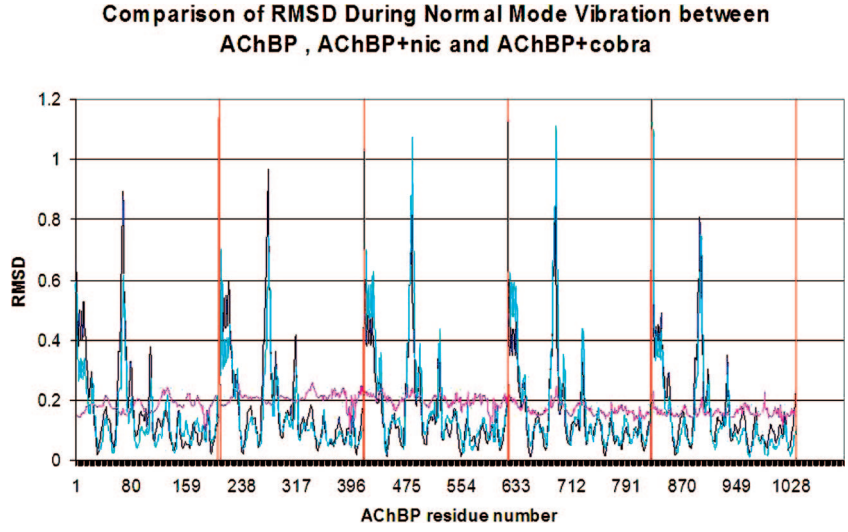

Figure 3. Plot of the normal mode trajectory motion as an α carbon rmsd vs residue number within the AChBP. AChBP (blue), AChBP+5nic (cyan), and AChBP+5cobra (pink). Notice the nearly identical motion of AChBP and AChBP+5nic but the extraordinarily dampened motion of AChBP within AChBP+cobra. Individual subunit extents are demarcated by the red vertical lines.

comes from the allosteric Monod-Wyman-Changeux models of the LGIC function which actually imply that agonist binding does not change receptor structure. In these models, an agonist acts simply by binding with higher affinity to the open state vs the closed state, shifting the pre-existing equilibrium between states toward the open state without inducing a change in receptor structure. In this case, one may not expect the normal-mode analysis to reveal a large change due to ligand binding, only a change in the energy landscape over which the transition occurs but which is not calculated with elastic network techniques. Just such an effect has been computationally demonstrated by the recent work of Arora and Brooks.[35]

Elastic network derived normal-mode analyses reveal an axially symmetric motion that is within the first few nontrivial, low frequency, high amplitude vibrations of the AChBP. It is a "blossoming-like" motion that involves the outward tilting of each subunit away from the axis

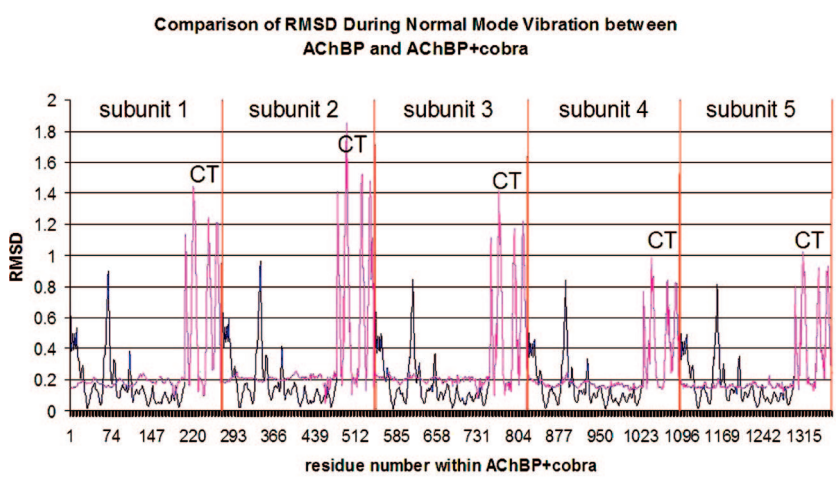

Figure 4. Plot of the normal mode trajectory motion as an α carbon rmsd vs residue number from AChBP+5cobra. AChBP (blue) and AChBP+5cobra(pink). Notice the extraordinarily dampened motion of the AChBP portion within AChBP+5cobra and the markedly exaggerated motion within the cobratoxin (CT) itself. Individual subunit extents are demarcated by the red vertical lines.

spanning the central pore. This motion is similar to that postulated by both Unwin, for portions of the nAChR,[1,36] and by McCammon, for the second nontrivial normal mode of the whole nAChR.[28] They suggest that these vibrations may contribute to the gating motion within the homologous region of the nAChR. Furthermore, the normal-mode analysis on the AChBP+0cobra demonstrates the same irislike wringing motion noted by ourselves and the others noted above, as present and consistent with channel gating in full models of LGICs. This lends further argument in favor of using the AChBP as a representative of possible relevant activities within the full nAChR. Our results clearly demonstrate that cobratoxin binding to the AChBP and AChBP+0cobra significantly dampens this motion. Since the function of cobratoxin is associated with an inhibitory effect on the nAChR, one may infer that the blunting of such channel-opening like motion is responsible for the overall effect of cobratoxin on ion channel conductance.

While the axially symmetric blossoming motion described here is distinctly different from the "irislike" gating motion also thought to be involved in ion channel opening, both may contribute to the overall gating function within the full structure of a LGIC. The irislike motion has been described by our laboratory for the homologous glycine alpha one and GABARa receptors[18,20] as well as in the work of Changeux[25] and McCammon[28] for the nAChR. Interestingly, the irislike gating motion appears to be produced only in a normal-mode analysis of the more complete model of a LGIC that includes both ligand binding and transmembrane domains or in AChBP+0cobra (slightly altered by the initial presence of cobratoxin) and not in the analysis of the ligand binding domain alone.[18]

The present work is among the first to demonstrate the effect of ligand binding on the natural functional motion of a protein, in particular a motion that may be homologous to the gating motion within a LGIC. In the future, it seems reasonable that if the protein motion associated with a protein's function can be discerned from normal-mode analyses, such analyses could become an additional, refined criterion in the final stages of a computational search for effective new drugs. However, when it comes to nonpeptide drugs containing far fewer atoms, using the effects of bound ligand on protein motion as additional criteria for drug design may require a more robust molecular mechanics treatment of the ligand–receptor complex.[20]

ACKNOWLEDGMENT

This work was supported by the Department of Veterans Affairs, the Stanford University School of Medicine, and the National Institutes of Health grants GM064371 and AA013378.

Supporting Information Available: MPEG movies of the relevant vibrational modes of AChBP and AChBP+5cobra as viewed down their pores. This material is available free of charge via the Internet at http://pubs.acs.org.

REFERENCES AND NOTES

(1) Miyazawa, A.; Fujiyoshi, Y.; Unwin, N. Structure and gating mechanism of the acetylcholine receptor pore. *Nature* **2003**, *424*, 949–55.
(2) Unwin, N. Refined structure of the nicotinic acetylcholine receptor at 4A resolution. *J. Mol. Biol.* **2005**, *346*, 967–89.
(3) Tsai, J.; Gerstein, M.; Levitt, M. Simulating the minimum core for hydrophobic collapse in globular proteins. *Protein Sci.* **1997**, *6*, 2606–2616.
(4) Brejc, K.; van Dijk, W. J.; Klaassen, R. V.; Schuurmans, M.; van Der Oost, J.; Smit, A. B.; Sixma, T. K. Crystal structure of an ACh-binding protein reveals the ligand-binding domain of nicotinic receptors. *Nature* **2001**, *411*, 269–76.
(5) Smit, A. B.; Brejc, K.; Syed, N.; Sixma, T. K. Structure and function of AChBP, homologue of the ligand-binding domain of the nicotinic acetylcholine receptor. *Ann. N. Y. Acad. Sci.* **2003**, *998*, 81–92.
(6) Celie, P. H.; van Rossum-Fikkert, S. E.; van Dijk, W. J.; Brejc, K.; Smit, A. B.; Sixma, T. K. Nicotine and carbamylcholine binding to nicotinic acetylcholine receptors as studied in AChBP crystal structures. *Neuron* **2004**, *41*, 907–14.
(7) Celie, P. H.; Kasheverov, I. E.; Mordvintsev, D. Y.; Hogg, R. C.; van Nierop, P.; van Elk, R.; van Rossum-Fikkert, S. E.; Zhmak, M. N.; Bertrand, D.; Tsetlin, V.; Sixma, T. K.; Smit, A. B. Crystal structure of nicotinic acetylcholine receptor homolog AChBP in complex with an alpha-conotoxin PnIA variant. *Nat. Struct. Mol. Biol.* **2005**, *12*, 582–8.
(8) Ulens, C.; Hogg, R. C.; Celie, P. H.; Bertrand, D.; Tsetlin, V.; Smit, A. B.; Sixma, T. K. Structural determinants of selective alpha-conotoxin binding to a nicotinic acetylcholine receptor homolog AChBP. *Proc. Natl. Acad. Sci. U.S.A.* **2006**, *103*, 3615–20.
(9) Bourne, Y.; Talley, T. T.; Hansen, S. B.; Taylor, P.; Marchot, P. Crystal structure of a Cbtx-AChBP complex reveals essential interactions between snake alpha-neurotoxins and nicotinic receptors. *Embo J.* **2005**, *24*, 1512–22.

(10) Levitt, M.; Sander, C.; Stern, P. S. Protein normal-mode dynamics: trypsin inhibitor, crambin, ribonuclease and lysozyme. *J. Mol. Biol.* **1985**, *181*, 423–47.
(11) Go, N.; Noguti, T.; Nishikawa, T. Dynamics of a small globular protein in terms of low-frequency vibrational modes. *Proc. Natl. Acad. Sci. U.S.A.* **1983**, *80*, 3696–700.
(12) Brooks, B.; Karplus, M. Harmonic dynamics of proteins: normal modes and fluctuations in bovine pancreatic trypsin inhibitor. *Proc. Natl. Acad. Sci. U.S.A.* **1983**, *80*, 6571–5.
(13) Hinsen, K. Analysis of domain motions by approximate normal mode calculations. *Proteins* **1998**, *33*, 417–29.
(14) Atilgan, A. R.; Durell, S. R.; Jernigan, R. L.; Demirel, M. C.; Keskin, O.; Bahar, I. Anisotropy of fluctuation dynamics of proteins with an elastic network model. *Biophys. J.* **2001**, *80*, 505–15.
(15) Tama, F.; Valle, M.; Frank, J.; Brooks, C. L. 3rd. Dynamic reorganization of the functionally active ribosome explored by normal mode analysis and cryo-electron microscopy. *Proc. Natl. Acad. Sci. U.S.A.* **2003**, *100*, 9319–23.
(16) Suhre, K.; Sanejouand, Y. H. On the potential of normal-mode analysis for solving difficult molecular-replacement problems. *Acta Crystallogr. D: Biol. Crystallogr.* **2004**, *60*, 796–9.
(17) Delarue, M.; Sanejouand, Y. H. Simplified normal mode analysis of conformational transitions in DNA-dependent polymerases: the elastic network model. *J. Mol. Biol.* **2002**, *320*, 1011–24.
(18) Bertaccini, E. J.; Trudell, J. R.; Lindahl, E. Normal Mode Analysis Reveals the Channel Gating Motion within a Ligand Gated Ion Channel Model. In *7th International Conference on Basic and Systematic Mechanisms of Anesthesia*; Elsevier: Nara, Japan, 2005; Vol. 1283, pp 160–163.
(19) Berman, H. M.; Westbrook, J.; Feng, Z.; Gilliland, G.; Bhat, T. N.; Weissig, H.; Shindyalov, I. N.; Bourne, P. E. The Protein Data Bank. *Nucleic Acids Res.* **2000**, *28*, 235–42.
(20) Bertaccini, E.; Trudell, J. R.; Lindahl, E. Successful calculation of glycine receptor gating motion via a full molecular mechanics force field. *Anesthesiology* **2006**, *105*, A175.
(21) Tirion, M. M. Large amplitude elastic motions in proteins from a single-parameter, atomic analysis. *Phys. Rev. Lett.* **1996**, *77*, 1905–1908.
(22) Bertaccini, E. J.; Trudell, J. R.; Lindahl, E. Normal-mode analysis of the glycine alpha1 receptor by three separate methods. *J. Chem. Inf. Model.* **2007**, *47*, 1572–9.
(23) Van Der Spoel, D.; Lindahl, E.; Hess, B.; Groenhof, G.; Mark, A. E.; Berendsen, H. J. GROMACS: fast, flexible, and free. *J. Comput. Chem.* **2005**, *26*, 1701–18.
(24) Guex, N.; Peitsch, M. C. SWISS-MODEL and the Swiss-PdbViewer: an environment for comparative protein modeling. *Electrophoresis* **1997**, *18*, 2714–23.
(25) Taly, A.; Delarue, M.; Grutter, T.; Nilges, M.; Le Novere, N.; Corringer, P. J.; Changeux, J. P. Normal mode analysis suggests a quaternary twist model for the nicotinic receptor gating mechanism. *Biophys. J.* **2005**, *88*, 3954–65.
(26) Brooks, B.; Karplus, M. Normal modes for specific motions of macromolecules: application to the hinge-bending mode of lysozyme. *Proc. Natl. Acad. Sci. U.S.A.* **1985**, *82*, 4995–9.
(27) Szarecka, A.; Xu, Y.; Tang, P. Dynamics of heteropentameric nicotinic acetylcholine receptor: Implications of the gating mechanism. *Proteins* **2007**, *68*, 948–60.
(28) Cheng, X.; Lu, B.; Grant, B.; Law, R. J.; McCammon, J. A. Channel opening motion of alpha7 nicotinic acetylcholine receptor as suggested by normal mode analysis. *J. Mol. Biol.* **2006**, *355*, 310–24.
(29) Hung, A.; Tai, K.; Sansom, M. S. Molecular dynamics simulation of the M2 helices within the nicotinic acetylcholine receptor transmembrane domain: structure and collective motions. *Biophys. J.* **2005**, *88*, 3321–33.
(30) Shrivastava, I. H.; Bahar, I. Common mechanism of pore opening shared by five different potassium channels. *Biophys. J.* **2006**, *90*, 3929–40.
(31) Valadie, H.; Lacapere, J. J.; Sanejouand, Y. H.; Etchebest, C. Dynamical properties of the MscL of Escherichia coli: a normal mode analysis. *J. Mol. Biol.* **2003**, *332*, 657–74.
(32) Karlin, A. A touching picture of nicotinic binding. *Neuron* **2004**, *41*, 841–2.
(33) Dellisanti, C. D.; Yao, Y.; Stroud, J. C.; Wang, Z. Z.; Chen, L. Crystal structure of the extracellular domain of nAChR alpha1 bound to alpha-bungarotoxin at 1.94 A resolution. *Nat. Neurosci.* **2007**, *10*, 953–962.
(34) Williamson, P. T.; Verhoeven, A.; Miller, K. W.; Meier, B. H.; Watts, A. The conformation of acetylcholine at its target site in the membrane-embedded nicotinic acetylcholine receptor. *Proc. Natl. Acad. Sci. U.S.A.* **2007**, *104*, 18031–18036.
(35) Arora, K.; Brooks, C. L., III. Large-scale allosteric conformational transitions of adenylate kinase appear to involve a population-shift mechanism. *Proc. Natl. Acad. Sci. U.S.A.* **2007**, *104*, 18496–501.
(36) Unwin, N. Structure and action of the nicotinic acetylcholine receptor explored by electron microscopy. *FEBS Lett.* **2003**, *555*, 91–5.

CI700456S